Catalysis Today 141 (2009) 125–129

Contents lists available at ScienceDirect

Catalysis Today

journal homepage: www.elsevier.com/locate/cattod

Acidity and catalytic activities of sulfated zirconia inside SBA-15

Shelu Garg [a], Kapil Soni [a], G. Muthu Kumaran [a], Rajaram Bal [a], Kinga Gora-Marek [b], J.K. Gupta [a], L.D. Sharma [a], G. Murali Dhar [a,*]

[a] Catalytic Conversion Processes Division, Indian Institute of Petroleum, Dehradun, India
[b] Faculty of Chemistry, Jagiellonian University, 30-060, Krakow, Ingardena 3, Poland

ARTICLE INFO

Article history:
Available online 15 May 2008

Keywords:
Sulfated zirconia
Brönsted acidity
SBA-15
ZrO_2-SBA-15
IR pyridine adsorption
Cumene cracking

ABSTRACT

SBA-15 containing various amount (10–50 wt.%) of highly dispersed ZrO_2 is prepared using urea hydrolysis method. The sulfated zirconia (ZrO_2) in SBA-15 catalysts were prepared using these materials. The materials were characterized by XRD, BET surface area, TEM, TGA, acidity measurements using in situ IR pyridine adsorption, sulfate content and catalytic activities were studied for cumene cracking and esterification of cyclohexanol. The Brönsted acidity, catalytic activity for cumene cracking and esterification and sulfate content were found to pass through a maxima where ZrO_2 loading is 35 wt.%. The 35SZ-SBA catalysts exhibited 6.4 times higher activity for cumene cracking compared to the bulk SZ catalysts. The relationship between acidity, sulfate content and catalytic activity are discussed in the light of existing knowledge on sulfated zirconia.

1. Introduction

In petroleum refining, environmental clean technologies are always been sought due to the stringent environmental regulations [1,2]. There are many industrially important acid catalyzed processes such as alkylation of isobutanes with butenes [3], isomerization of *n*-butane to isobutane [4] which are presently using liquid acids such as HF, H_2SO_4, $AlCl_3$, and BF_3, having unavoidable drawbacks due to corrosive nature and environmental problems. Solid acid seems to be a preferred alternative to the present liquid acid based technologies and significant efforts have already been made to develop solid acid catalysts for this application [5]. Sulfated zirconia (SZ) has been studied with great interest towards this end [6,7].

Sulfated zirconia (SZ) possesses both strong Brönsted and Lewis acid sites depending on the preparation condition. Due to its strongly acidic nature, SZ finds application in many industrially important reactions such as hydrocarbon isomerization, alkylation, and esterification [6]. Many authors investigated the nature of acidity of SZ and their origin using XPS and thermal characterization techniques [8]. It was proposed that the active site consists of poly sulfate species comprising of three or four oligomers with two ionic bonds of S–O–Zr in addition to coordination bonds of S=O with Zr [8]. However, the relatively low surface area and smaller pore size of SZ prepared under conventional methods limits their potential applications.

To overcome this, many approaches have been pursued like preparing nanosized sulfated zirconia with high surface area (165 m^2/g) and pore volume of 0.34 cm^3/g. Chen et al. [9] prepared SZ supported on mesoporous MCM-41 with sulfur content up to 4.95 wt.% and demonstrated that very high catalytic activity for *n*-butane isomerization compared to SZ/SiO_2 catalyst. In a similar work, Kawi and co-workers [10] synthesized SZ over MCM-41 (super acid catalyst) with sulfate content of 5.8–7.6 wt.% by post synthetic chemical liquid deposition method, followed by hydrolysis of zirconium propoxide. This solid super acid found to be 2–3 times more active than the conventional SZ for MTBE synthesis and *n*-pentane isomerization. Recently, Zhao et al. [11] Synthesized Sulfated zirconia supported on mesoporous γ-Al_2O_3 and found that this mesoporous solid acid exhibits superior catalytic performance to sulfated zirconia and MCM-41 supported sulfated zirconia towards conversion of *n*-pentane, Friedel-Craft benzoylation of anisole. Landau et al. [12] made an attempt to prepare thermally stable and catalytically active tetragonal ZrO_2 in nanotubes of SBA-15 by chemical solution decomposition method and reported 1.5–2.2 times increase in catalytic activity per gm of SZ-SBA-15 for dehydration of isopropanol compare with regular bulk SZ material. The nature of acidity of SZ can vary with slight change in the preparation methods. Many reports suggested that the strong acid sites were associated with sites of low coordination such as defects, corners or edges at the surface of small particles. Therefore, a detailed study on acidity characterization and their correlation with catalytic activity of SZ on mesoporous supports may enhance

* Corresponding author. Tel.: +91 135 2660146; fax: +91 135 2660202.
E-mail address: gmurli@iip.res.in (G.M. Dhar).

0920-5861/$ – see front matter © 2008 Elsevier B.V. All rights reserved.
doi:10.1016/j.cattod.2008.03.021

our understanding of the acid catalysis on sulfated zirconia (SZ). With this aim, in this communication, we systematically varied the ZrO_2 content in mesoporous SBA-15 by post synthetic homogenous urea hydrolysis method, followed by sulfation, for preparing sulfated ZrO_2. The materials were characterized with XRD, TEM, TGA, and pore size distribution. Acidity characterization was done on both ZrO_2-SBA and SZ/SBA using FT-IR pyridine adsorption method. The catalytic activity of both ZrO_2-SBA and SZ/SBA was studied using cumene cracking and esterification of cyclohexanol. Correlation between the acidity and catalytic activity of various SZ samples was also investigated.

2. Experimental

2.1. Preparation of catalysts

Mesoporous SBA-15 was prepared according to published literature and the detailed procedure described elsewhere [13]. The final calcined SBA-15 material was dried at 393 K and used for post-synthetic treatment. ZrO_2 deposition at various wt.% (10–50 wt.%) was carried out using SBA-15 by homogeneous urea hydrolysis method. In a typical synthesis (10 wt.% ZrO_2), 4.0 g of dried SBA-15 was immersed in 120 ml of distilled water containing 1.1622 g of Zirconiumoxychloride ($ZrOCl_2{\cdot}8H_2O$, Aldrich) and 1.083 g of urea. The mixture was refluxed at 363 K for 5–6 h (pH ~8) and the resultant gel was filtered followed by repeated washing with distilled water to remove excess chloride ions. The filtered ZrO_2-SBA gel was dried in air and at 383 K for 24 h followed by calcination in air at 823 K for 6 h. Pure ZrO_2 was also prepared for comparison purpose using the same method as above.

Sulfation of various ZrO_2 containing SBA-15 samples was carried out by stirring with 1(N) H_2SO_4 (15 ml/g) at room temperature for 3 h, and the resultant material was filtered and dried at 383 K followed by calcination in air at 823 K for 3 h. The ZrO_2 containing SBA-15 and their corresponding sulfated samples were designated as (*X*)ZrO_2-SBA, (*X*)SZ-SBA, respectively, where (*X*) stands for theoretical wt.% of ZrO_2 in SBA-15.

2.2. Characterization

The calcined mesoporous SBA-15, (X)ZrO_2-SBA, and (*X*)SZ-SBA samples were characterized by low-angle X-ray diffraction (XRD), N_2 adsorption analysis, Transmission electron microscopy (TEM), CO_2 chemisorption, wide-angle X-ray analysis, FT-IR of pyridine adsorption, TGA/DTA, etc. N_2 adsorption analysis was carried out using micromeritics (ASAP-2010) at liquid nitrogen temperature (77 K). To know the actual surface area of ZrO_2 in (*X*)ZrO_2-SBA samples, the CO_2 chemisorption at room temperature (298 K) was performed, the CO_2 uptakes on (*X*)ZrO_2-SBA were normalized using pure ZrO_2 for knowing the surface area of ZrO_2 (EZSA) in (*X*)ZrO_2-SBA samples. Thermo gravimetric analysis (TGA) was carried out on calcined pure SZ and (*X*)SZ-SBA samples and evaluated the amount of sulfate species that are present on them.

FT-IR pyridine adsorption was used to distinguish the Brönsted and Lewis acidity of various (*X*)ZrO_2-SBA, and (*X*)SZ-SBA samples. The excess of pyridine was adsorbed at 400 K, and physisorbed molecules were subsequently removed by evacuation at the same temperature. The concentration of Brönsted and Lewis acid sites was calculated from the intensities of 1545 cm^{-1} band for PyH^+ and of 1450 cm^{-1} band for PyL. The values of extinction coefficients were determined in the experiments in which measured portions of pyridine were adsorbed on H-Mordenite (containing only Brönsted acid sites) or on Al_2O_3 (containing only surface Lewis acid sites).

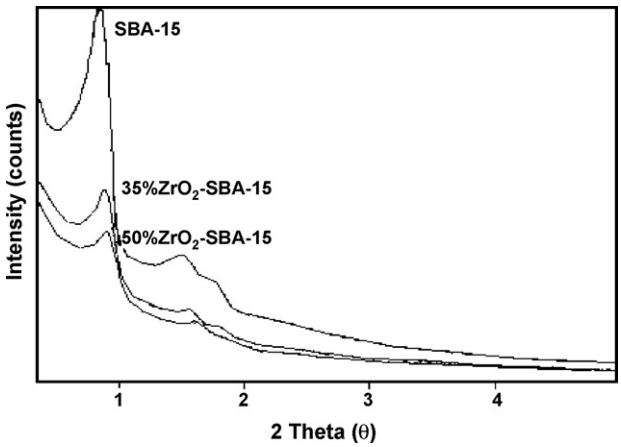

Fig. 1. Low-angle XRD patterns of catalysts: SBA-15, 35%ZrO_2-SBA-15 and 50%ZrO_2-SBA-15.

2.3. Catalytic activity

Cumene cracking activity on various (*X*)ZrO_2-SBA, and (*X*)SZ-SBA samples were evaluated in a fixed-bed catalytic micro reactor operating at atmospheric pressure and interfaced with six-way sampling valve to a gas chromatograph for on-line product analysis. The first order rates were evaluated according to equation $x = r(W/F)$, where r is rate in mol h^{-1} g^{-1}, x is the fractional conversion, W is the weight of the catalyst in grams and F is the flow rate of reactant in mol h^{-1}. The conversions were kept below 15% to avoid diffusional limitations [14]. Catalytic esterification of cyclohexanol with acetic acid was performed at 373 K in a round bottom flask. During the experiment, acetic acid was always used in stoichiometric excess over the reactant alcohol. The details of the procedure described elsewhere [15].

3. Results and discussion

3.1. Low-angle X-ray diffraction

SBA and (*X*)ZrO_2-SBA samples show three well-resolved diffraction peaks correspond to $d_{1\,0\,0}$, $d_{1\,1\,0}$, and $d_{2\,0\,0}$ planes characteristics of *P6mm* hexagonal mesoporous material (Fig. 1). There is slight upward shift in the 2θ value with ZrO_2 content in SBA indicates the added ZrO_2 causes minor changes in the unit cell parameter of SBA. This is probably due to minor shrinkage in the pore walls of SBA with addition of ZrO_2. The intensity of all three diffraction pattern ($d_{1\,0\,0}$, $d_{1\,1\,0}$, $d_{2\,0\,0}$) decreases with increasing ZrO_2 content in SBA indicate the ZrO_2 addition causes partial structural collapse that is predominant at 50 wt.%. Wide-angle XRD was carried out on all (*X*)ZrO_2-SBA and (*X*)SZ-SBA samples and found that none of crystalline peaks due to ZrO_2 are seen in the wide-angle region (10–80 2θ) suggesting that there is no bigger crystallite formation of ZrO_2 even after addition of 50 wt.% ZrO_2 and calcination at 823 K.

Table 1
Textural characterization of SBA-15 and SZ-SBA-15

Sample	S_{BET} (m^2/g)	Total pore volume (cm^3/g)	Mean pore diameter (Å)
SBA-15	696	0.96	66.3
35%ZrO_2-SBA-15	375	0.69	48.3
35%SZ-SBA-15	325	0.52	45.1

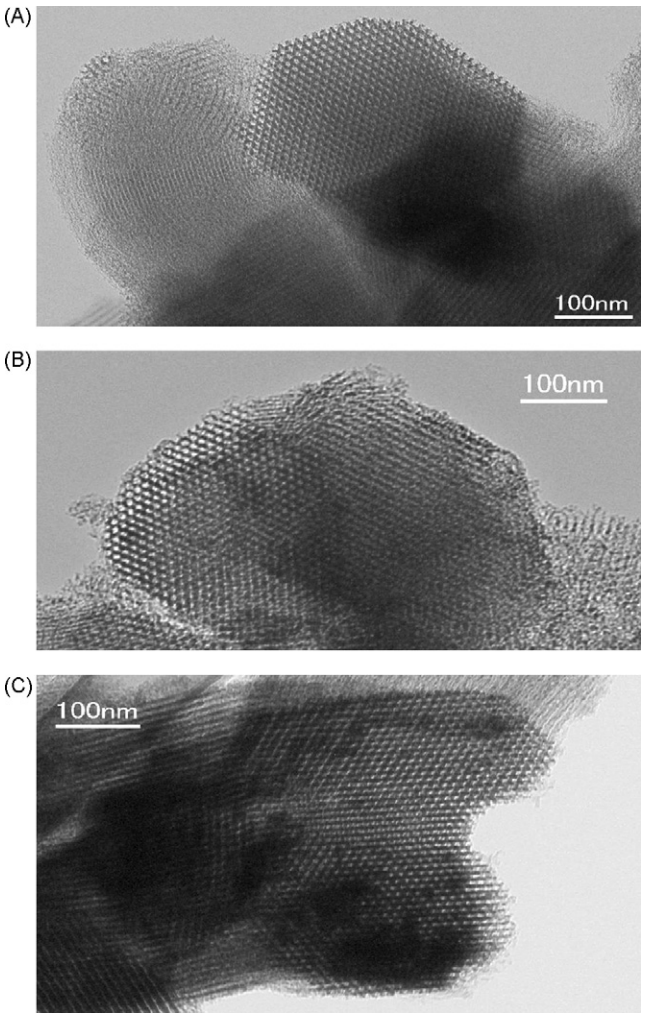

Fig. 2. TEM micrographs of (A) SBA-15, (B) 35%ZrO_2-SBA, (C) 35%SZ-SBA.

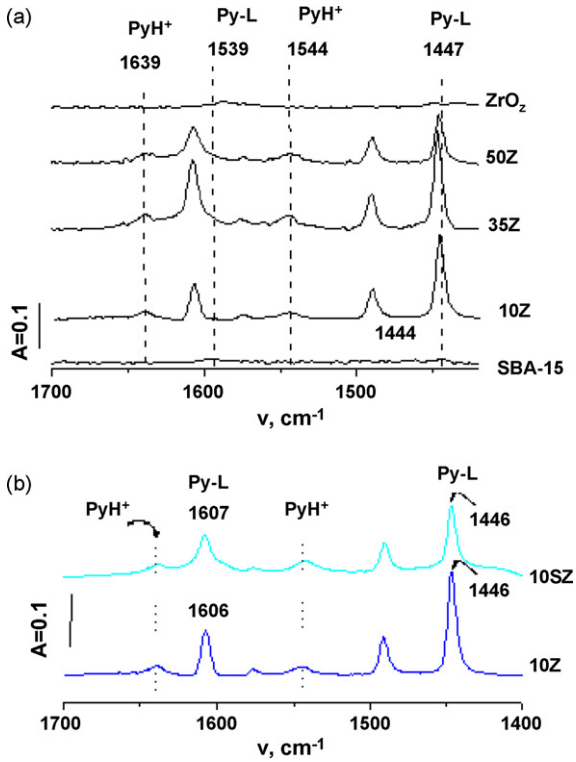

Fig. 3. The IR spectra of pyridine adsorbed species on (a) SBA-15 and (*X*)ZrO_2-SBA, (b) 10%ZrO_2-SBA and 10%SZ-SBA.

observation that the SZ is highly dispersed in the interior surface of the mesopores of MCM-41 by following the decreasing trend of mean pore diameter of MCM-41 with zirconia addition. The HRTEM results shown in Fig. 2, clearly show that in the case of SBA-15, ZrO_2-SBA-15 and SZ-SBA-15 the hexagonal mesoporous structure is preserved after ZrO_2 addition and subsequent sulfation indicating that, the structural integrity is maintained after all these treatments.

3.2. N_2 adsorption analysis

Nitrogen adsorption analysis was carried out on SBA, (*X*)ZrO_2-SBA, and (*X*)SZ-SBA samples and the typical results are shown in Table 1. SBA-15, 35ZrO_2-SBA and 35SZ-SBA show typical type-IV isotherm with H_1 hysteresis loop, observing that the height of hysteresis loop decreases with addition of 35% SZ reflecting from the decrease in total pore volume and mean pore diameter shown in Table 1. BET surface area and total pore volume decreases from 696 to 325 m^2/g and 0.96 to 0.52 cm^3/g, respectively, after addition of 35SZ to SBA indicates the added SZ could be mainly located inside the SBA mesoporous channels. The mean pore diameter of SBA decreases from 66.3 to 45.1 Å with 35SZ addition also supports the above said conclusion. Chen et al. [9] also made a similar

3.3. Acidity characterization

Infrared spectroscopic studies of pyridine adsorption on solid surfaces have made it possible to distinguish between Brönsted and Lewis acid sites [16]. Table 2 shows the infrared spectra of pyridine adsorption on SZ and (*X*)SZ-SBA samples evacuated at 400 K. The band at 1545 cm^{-1} for Brönsted acidity increases with increasing ZrO_2 in SZ-SBA samples, reaches maximum at 35 wt.% and then falls. In fact, the total acidity also follows the similar trend as Brönsted acidity. On the other hand, the band at 1450 cm^{-1} for Lewis acidity continuously falls with ZrO_2 content in SZ-SBA as shown in Fig. 3.

In the same figure, pyridine adsorption patterns of 10ZrO_2-SBA and 10SZ-SBA are also shown. It can be seen that there exists clear

Table 2
The concentration of Brönsted and Lewis acid sites determined with pyridine in materials studied

Sample	PyH^+ (μmol/g)	PyL (μmol/g)	PyL + PyH^+ (μmol/g)	$A_{530\ K}/A_{400\ K}$ PyL	$A_{530\ K}/A_{400\ K}$ PyH^+
ZrO_2	–	20	20	0	–
10%ZrO_2-SBA-15	70	585	655	0.55	0.65
35%ZrO_2-SBA-15	105	700	805	0.65	0.53
50%ZrO_2-SBA-15	80	385	475	0.45	0.45
$SZrO_2$	0	0	0	–	–
10%SZ-SBA-15	85	365	450	0.84	0.58
35%SZ-SBA-15	280	300	580	0.66	0.68
50%SZ-SBA-15	110	300	410	0.57	0.42

Table 3
Cumene cracking and esterification activity

	S_{BET} (m^2/g)	SO_4^{-2} (wt.%)	SO_4^{-2}/EZSA[a]	Rate of reaction	
				Cumene cracking ($\times 10^{-3}$ mol h^{-1} g^{-1})	Esterification (% conversion)
SBA-15	696	–	–	11.92	Nil
10%SZ-SBA-15	430	6.47	0.07	213.5	44.66
35%SZ-SBA-15	352	14.77	0.25	467.5	52.02
50%SZ-SBA-15	198	2.11	0.03	120.5	23.6
SZ pure	80	12.03	–	72.77	20.5

[a] EZSA (equivalent zirconia surface area) calculated from CO_2 adsorption.

evidence for the presence of Brönsted and Lewis acid sites. A comparative analysis of pyridine adsorption data on Zr-SBA-15 containing various amounts of ZrO_2 and their sulfated analogues are shown in Table 2. It can be seen that both Lewis and Brönsted acid sites passes through a maximum at 35 wt.% ZrO_2 in SBA-15, both in the case of ZrO_2 and its sulfated analogues. The last column of the Table 2 showing relative ratio of Brönsted sites that are present at 530 K relative to 400 K shows a similar trend. These values represent strong Lewis and Brönsted acid sites. These strong acid site concentration is maximum at 35 wt.% ZrO_2 in the sulfated analogue. It is interesting to note that 35SZ-SBA-15 contains larger number of strong acid sites compared to unsulfated analogues. It is also interesting to note that on sulfated ZrO_2 the Lewis acid site concentration decreases and the Brönsted acid site concentration increases compared to unsulfated ones suggesting that some of the Lewis acid sites are converted to Brönsted acid sites during sulfation.

The type of sulfate species that exist on the ZrO_2 support and their contributions to acidity is always a controversy. Hino et al. [8] suggested three structural model of sulfated zirconia, namely mono sulfate, cyclic trimer, and poly sulfate species composing of mainly three or four oligomers. They contain both Brönsted and Lewis acid sites depending on the preparation conditions and pretreatment. Fraenkel [17] suggested that SZ with an effective super acid should contain a critical amount of moisture and this moisture can play an important role in reversible transformation of Brönsted and Lewis acidity.

3.4. Catalytic activity

Catalytic activity of pure SZ and SZ-SBA-15 samples were evaluated for cumene cracking and esterification of cyclohexanol using acetic acid. The detailed experimental procedure is described in literature [15]. The first order rates were evaluated for Cumene cracking at 473 K for all SZ catalysts and shown in Table 3. SBA-15 support shows only minor cracking activity (11.9×10^{-3} mol h^{-1} g^{-1}) and the rate of reaction increases with increasing Zirconia content in SBA up to 35 wt.% ZrO_2 and start falling at 50 wt.%. 35SZ-SBA Exhibit 6.4 times higher cracking activity than the pure SZ prepared under similar conditions. Activity for esterification of cyclohexanol was measured in terms of % conversion of cyclohexanol after 4 h and shown in Table 3. Pure SBA does not display any activity and there is steep increase in conversion (52%) with increase of SZ up to 35 wt.% and then decreases to 23.6 in the case of 50SZ-SBA. The extent of increment in esterification of cyclohexanol with increase of SZ is less compared to cumene cracking probably due to the fact that the esterification needs stronger acidity.

Fig. 4 shows a comparison of acidity and catalytic activity for cumene cracking as well as esterification, with acidity and sulfate concentration on the samples. It can be seen that the catalytic activity for cumene cracking as well as esterification passes a maximum at around 35SZ-SBA-15. The Brönsted acidity shown in the same figure also passes through the maximum at 35SZ-SBA-15. The sulfate uptake also passes through the maximum at the same point viz 35SZ-SBA-15. It appears that the strong Brönsted acid sites generated on SZ-SBA-15 by sulfation are indeed predominantly responsible for the above reactions on these catalysts. The data on SO_4/EZSA (Equivalent Zirconia Surface Area) which represents sulfate ions per unit Zirconia area, also exhibits a maximum at 35SZ-SBA-15 suggesting that highest sulfate content per unit area results in higher activity which in turn means that sulfate moieties containing more than one sulfate species are likely to be part of active sites. However, the fact that Lewis acid sites variation with ZrO_2 content is different compared to Brönsted acid sites and catalytic activity variation suggest, that Brönsted acidity of sulfated ZrO_2 inside SBA-15 predominantly controls the catalytic properties for the two reactions.

Relative catalytic performance of SZ-SBA-15 for cumene cracking activities in comparison to other acidic materials like

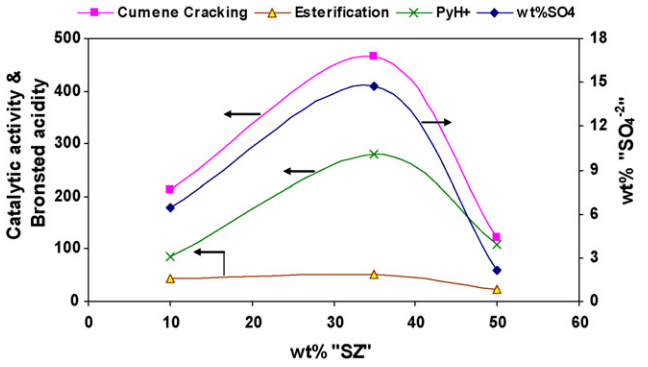

Fig. 4. Variation of catalytic activity, Brönsted acid sites and sulfate content with wt.% of ZrO_2 loading in SZ-SBA. Units of Cumene cracking ($\times 10^{-3}$ mol h^{-1} g^{-1}), esterification (% conversion) and Brönsted acidity (mol g^{-1}).

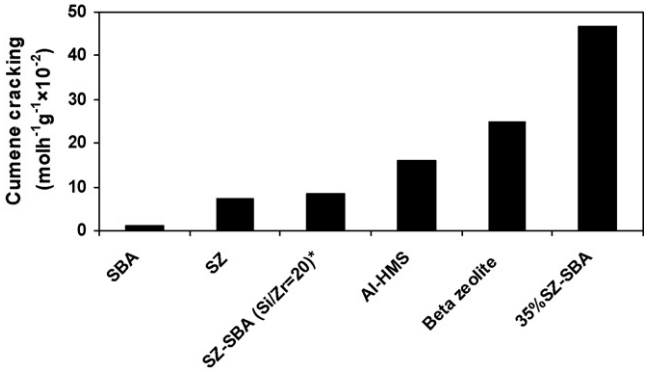

Fig. 5. Comparison of cumene cracking activity of various solid acid catalysts.

pure SBA-15, sulfated Zirconia, sulfated Zirconia in the SBA-15 structure (SZ-SBA-15, Si/Zr = 20), Al-HMS, Beta Zeolite and 35SZ-SBA-15 are shown in Fig. 5. It can be seen that 35SZ-SBA-15 is superior to all these acidic materials in catalytic performance for this particular reaction. The activity of 35SZ-SBA-15 is 6.4 times more than sulfated Zirconia. It can be inferred from the above results that the surface area of ZrO_2 inside SBA-15 and its ability to hold SO_4^{-2} ion to create strongly acidic sites are key factor in determining the catalytic activity.

4. Conclusions

The SBA-15, ZrO_2-SBA-15 were synthesized with high surface area and ZrO_2 dispersion can be inferred from XRD, CO_2 adsorption, electron microscopy. These results also indicate that SBA-15 structural integrity is preserved except at highest loading studied. The acidity measurements showed evidence for presence of Brönsted and Lewis acid sites as a function of ZrO_2 loading and in their sulfated analogues. It is observed that some of the Lewis acid sites on ZrO_2 are converted to Brönsted acid sites after sulfation. The Brönsted acid sites passed through a maximum as a function of ZrO_2 on SBA-15 in the sulfated catalysts, while the Lewis acid sites continuously decreased. It appears that the Brönsted acid sites created after sulfation are responsible for the observed activity increase. The sulfate groups per unit ZrO_2 area indicated the active sites are likely to contain more than one sulfate groups in the active site.

Acknowledgements

The authors are grateful to The Director, Dr. M.O. Garg, Indian Institute of Petroleum for his constant encouragement and Shelu Garg and Kapil Soni thank CSIR, India for providing fellowship.

References

[1] C. Song, Catal. Today 86 (2003) 211.
[2] Y. Okamoto, M. Bressey, G. Murali Dhar, C. Song, Effect of support in hydrotreating catalysis for ultra clean fuels, Catal. Today 86 (2003) 1.
[3] A. Feller, J.A. Lercher, Adv. Catal. 48 (2004) 229.
[4] G.A. Olah, G.K.S. Prakash, J. Sommer, Superacids, Wiley-Interscience, NY, USA, 1985, p. 33.
[5] A. Platon, W.J. Thomson, Appl. Catal. A: Gen. 282 (1 and 2) (2005) 93.
[6] K. Arata, Adv. Catal. 37 (1990) 165.
[7] M. Hino, K. Arata, J. Chem. Soc. Chem. Commun. (1980) 851.
[8] M. Hino, M. Kurashige, H. Matsuhashi, K. Arata, Thermochim. Acta 441 (2006) 35.
[9] C.-L. Chen, T. Li, S. Cheng, H.-P. Lin, C.J. Bhongale, C.-Y. Mou, Micropor. Mesopor. Mater. 50 (2001) 201.
[10] Q.-H. Xia, K. Hidajat, S. Kawi, Chem. Commun. (2000) 2229.
[11] J. Zhao, Y. Yue, W. Hua, H. He, Z. Gao, Catalytic activities and properties of sulfated zirconia supported on mesostructured γ-Al_2O_3, Appl. Catal. A: Gen. 336 (1–2) (2008) 133.
[12] M.V. Landau, L. Titelman, L. Vradman, P. Wilson, Chem. Commun. (2003) 594.
[13] Y. Yue, A. Gedeon, J. Bonardt, J. d'Espinose, N. Melosh, J. Fraissard, Chem. Commun. 19 (1999) 1967.
[14] M.S. Rana, B.N. Srinivas, S.K. Maity, G. Murali Dhar, T.S.R. Prasada Rao, J. Catal. 195 (2000) 31.
[15] Y. Sun, S. Ma, Y. Du, L. Yuan, S. Wang, J. Yang, F. Deng, F.S. Xiao, J. Phys. Chem. B 109 (2005) 2567.
[16] F. Babou, G. Coudurier, J.C. Vedrine, J. Catal. 152 (1995) 341.
[17] D. Fraenkel, Chem. Lett. (1999) 917.